Research in Health & Medical Sciences *Original Article*

2023 December; 2(4)

Photocatalytic Degradation of Azithromycin in Aqueous Solutions Using Magnetically Titanium-Iron Oxide Nanocomposites

Farnaz Heidarinejad[1]*, Hossein Kamani[1]

[1] Infectious Diseases and Tropical Medicine Research Center, Research Institute of Cellular and Molecular Sciences in Infectious Diseases, Zahedan University of Medical Sciences, Zahedan, Iran

***Corresponding Author Email: farnaz6505@gmail.com**
Received: 2025/9; Revised: 2025/9; Accepted: 2025/10

Abstract

Antibiotics, including Azithromycin, have been increasingly detected in the environment over recent decades, contributing to significant environmental pollution and posing risks to human health. This study aimed to evaluate the photocatalytic removal efficiency of Azithromycin from aqueous solutions using Fe-doped TiO_2@Fe_3O_4 nanocatalysts under a 30-W UVC lamp, two 15-W lamps with an irradiance of approximately 15mW/cm². The nanocatalysts were synthesized via a sol-gel method, with their properties confirmed through SEM, XRD, FTIR, and VSM analyses, verifying the incorporation of Fe ions into the TiO_2@Fe_3O_4 structure. The effects of key variables were investigated, including pH (3, 5, 7, 9, 11), initial Azithromycin concentration (50, 100, 150 mg/L), nanocatalyst dosage (500, 1000, 1500 mg/L), and reaction time (30, 60, 90 min). The maximum degradation efficiency of 95% was achieved at pH 3, an initial Azithromycin concentration of 50 mg/L, a catalyst dosage of 1000 mg/L, and a reaction time of 90 minutes. Given the high efficiency of this photocatalytic process, its application is recommended for the removal of Azithromycin from water resources.

Keywords: Azithromycin, photocatalytic degradation, Fe-doped TiO_2@Fe_3O_4, UV-C irradiation, sol-gel method

Introduction

In recent decades, antibiotics have been increasingly detected in various environmental compartments, contributing to significant pollution and posing risks to human health (1). Among these, Azithromycin stands out as one of the most widely used antibiotics globally, prescribed for treating infections caused by anaerobic bacteria and protozoa (2). It is also utilized in veterinary medicine to control parasites in livestock, poultry, and aquaculture feed (3). Due to its high chemical stability, resistance to biodegradation, and significant aqueous solubility, Azithromycin is poorly removed by conventional wastewater treatment processes (4)(5). This persistence leads to its accumulation in aquatic environments, where it exerts toxic, carcinogenic, and mutagenic effects on organisms and contributes to the rise of antimicrobial resistance (6)(7)(8). Therefore, the development of efficient strategies for the removal of Azithromycin from contaminated aquatic environments is essential to safeguard both environmental integrity and public health.

Antibiotics in water and wastewater pose a serious environmental challenge, and numerous treatment technologies have been explored to mitigate their impact (9). Conventional approaches such as adsorption, biological treatment, and membrane filtration are commonly used but often prove insufficient (10)(11)(12). Adsorbents can quickly lose capacity and require regeneration or disposal, membranes are vulnerable to fouling and costly maintenance, and biological systems are easily inhibited by the toxic nature of antibiotics (13)(14)(12). An alternative strategy involves oxidative processes. Traditional oxidation may only partially degrade contaminants, producing secondary pollutants that can remain hazardous. In contrast, advanced oxidation processes (AOPs) operate through the in situ generation of reactive oxygen species, predominantly hydroxyl radicals, which exhibit strong oxidative potential capable of degrading and mineralizing complex organic compounds. (15). This makes AOPs highly effective for the elimination of antibiotics and other persistent compounds (16). The development of nanotechnology-based solutions has added a new dimension to water purification. Engineered nanomaterials offer a large surface-to-volume ratio, tunable surface properties, and enhanced reactivity (17). Magnetic nanocomposites present notable advantages by combining high sorption capacity with magnetic separability, economic viability, reusability, and environmental compatibility, rendering them highly effective candidates for advanced water treatment technologies. These features make them more efficient and practical compared to many conventional adsorbents (18)(19). Among nanomaterials, iron nanoparticles have drawn attention due to their strong redox activity, enabling the removal of diverse pollutants, including halogenated organics, nitrates, pesticides, dyes, heavy metals, and antibiotics (20)(21)(22). Similarly, titanium dioxide (TiO_2) is currently the most extensively utilized photocatalyst in wastewater treatment, owing to its chemical stability, cost-effectiveness, non-toxic nature, and high photoactivity under UV irradiation. TiO2-based systems have consistently demonstrated high performance in degrading pharmaceutical residues (23)(23)(24).

The environmental persistence of antibiotics, particularly Azithromycin, in aquatic ecosystems presents a substantial threat to ecological balance and public health, thereby necessitating the development of effective treatment strategies. Titanium dioxide (TiO_2) is a widely utilized photocatalyst due to its chemical stability and strong oxidative potential; however, its practical performance is hindered by a wide band gap and rapid electron–hole recombination. The incorporation of iron oxide (Fe_2O_3) has been shown to effectively narrow the band gap, enhance charge carrier separation, and improve overall photocatalytic efficiency. Accordingly, this study aims to synthesize magnetically recoverable Fe-doped TiO_2@Fe_3O_4 nanocatalysts, characterize their physicochemical

properties, and assess their performance in the photocatalytic degradation of Azithromycin (AZM) from aqueous media.

Materials and methods

In this study, all chemicals were of analytical grade and used without further purification. Ferric chloride hexahydrate (FeCl3·6H2O), ferrous chloride tetrahydrate (FeCl2·4H2O), ferric nitrate ($Fe(NO_3)_3$), ammonia solution, ethanol, deionized water, nitric acid (HNO_3), titanium(IV) isopropoxide, sulfuric acid (H_2SO4), and sodium hydroxide (NaOH) were obtained from Merck (Germany). Azithromycin dihydrate ($C38H72N_2O12·2H2O$), used as the target contaminant in photocatalytic degradation experiments, was purchased from Sigma-Aldrich.

Synthesis of Magnetic Iron Oxide (Fe_3O_4) Nanocatalysts

Fe_3O_4 nanocatalysts were prepared by dissolving 5 g $FeCl_2•4H_2O$ and 4.71 g $FeCl_3•6H_2O$ in 200 mL of double-distilled water under stirring (600 rpm). Ammonia solution (1.5 mM) was added dropwise until pH > 8, forming a black precipitate. The reaction proceeded for 2 hours under a nitrogen atmosphere with continuous stirring. The product was washed repeatedly with distilled water and dried at room temperature to obtain the final nanocatalyst (25).

Synthesis of Fe-doped $TiO_2@Fe_3O_4$ Nanocatalysts

In this study, Fe-doped $TiO_2@Fe_3O_4$ and Fe-doped TiO_2 nanocatalysts were synthesized via the sol–gel method, known for producing uniform and highly reactive nanomaterials.

To begin, Fe $(NO_3)_3$, ethanol, deionized water, and HNO_3 were stirred to form solution 1. Separately, titanium (IV) isopropoxide, ethanol, and Fe_3O_4 nanoparticles were mixed to prepare solution 2. Solution 1 was added dropwise into solution 2 under stirring to initiate hydrolysis and condensation. After forming a homogeneous solution, the mixture was aged for 5 hours at room temperature. The resulting gel was washed, dried at 100°C for 2.5 hours, and calcined at 500°C for 1 hour to enhance crystallinity and photocatalytic performance (26).

Characterization of nanoparticles

The synthesized Fe-doped $TiO_2@Fe_3O_4$ nanocatalysts were extensively characterized to confirm their structural, morphological, magnetic, and compositional properties. Techniques such as scanning electron microscopy (SEM) and transmission electron microscopy (TEM) were used to observe particle size and morphology, X-ray diffraction (XRD) was employed to determine crystal structure, energy-dispersive X-ray spectroscopy (EDX) confirmed elemental composition, and vibrating sample magnetometry (VSM) was applied to evaluate magnetic properties. These comprehensive characterizations ensured that the nanocatalysts possessed the desired physicochemical properties for effective photocatalytic degradation of target contaminants such as azithromycin.

Photocatalytic Activity of Prepared Nanocatalysts

The photocatalytic degradation of azithromycin was investigated by evaluating the effects of pollutant concentration, Fe-doped $TiO_2@Fe_3O_4$ nanoparticle dosage, UV exposure time, and initial solution pH. Azithromycin solutions (1000 mL) were prepared at concentrations of 50, 100, and 150 mg/L, and the pH was adjusted to 3, 5, 7, 9, and 11 using 0.1 N NaOH or H2SO4. Fe-doped $TiO_2@Fe_3O_4$ nanocatalysts were added at doses of 500, 1000, and 1500 mg/L. The suspensions were stirred in the dark for 15 minutes to achieve adsorption–desorption equilibrium before UV-C irradiation using two 15-Watt lamps (Time contact: 30, 60, and 90 min). Samples were collected at regular intervals, and the nanocatalysts were separated before analysis. Azithromycin concentrations were measured using UV–Vis spectroscopy at 462 nm. The photocatalytic degradation efficiency was calculated as (26):

$$removal\ \% = \frac{C_i - C_o}{C_i} \times 100 \qquad (1)$$

C0 is the initial azithromycin concentration, and Ce is the concentration after irradiation. Optimal conditions were determined to maximize degradation efficiency under UV-C light.

Results and Discussion

SEM Analysis

Scanning Electron Microscopy (SEM) was used to examine the morphology and size distribution of the Fe-doped TiO_2@Fe_3O_4 nanocatalysts. The SEM images (Figure 1) reveal that the particles are generally well-formed, with sizes below 100 nm and predominantly smooth surfaces. Some aggregation is observed, which can be attributed to the fine particle size and the magnetic nature of the nanocatalysts. Overall, the images indicate a uniform morphology with discrete nanoparticles that occasionally cluster, reflecting both their nanoscale dimensions and inherent magnetic interactions. In the study by Tan et al., the microstructural analysis of TiO_2/Fe_3O_4 nanocomposites revealed no notable differences among the samples. The nanoparticles were predominantly spherical and of small size, with no significant aggregation observed in the SEM micrographs. The average particle size was determined to be 92.6 ± 7.2 nm, and the structures exhibited visible porosity, which could be beneficial for enhancing surface-related properties (27)

.

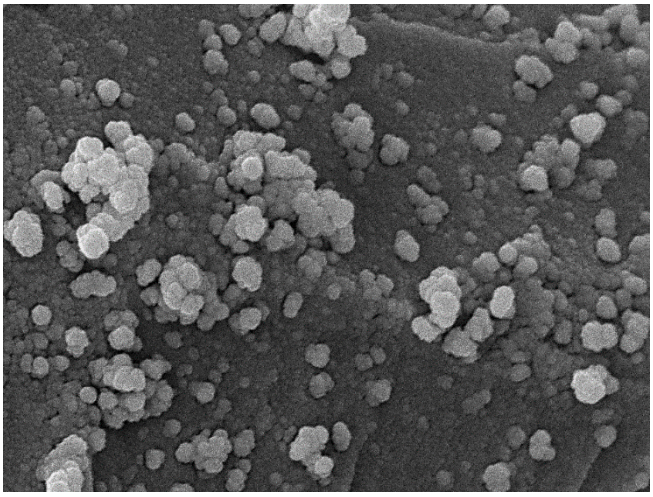

Figure 1. SEM images of Fe-doped TiO_2@Fe_3O_4 nanocatalysts. Scale bar: 200 nm

XRD Analysis

The X-ray diffraction (XRD) pattern of the Fe-doped TiO2@Fe3O4 nanocatalysts (Figure 2) displays sharp and well-defined peaks, indicating a highly crystalline structure. Reflections at 25.32°, 37.78°, 47.98°, 54.20°, 55.02°, 62.11°, and 69.21° validate the anatase phase. Minor peaks at 62.11°, 69.21°, 70.48°, and 75.23° indicate partial Fe^{3+} incorporation due to ionic radius similarity with Ti^{4+}, causing slight lattice distortion. This substitution stabilizes the anatase phase, limits rutile formation, and preserves photocatalytic efficiency (28).

VSM Analysis

Magnetic nanocatalysts exhibiting superparamagnetic behavior at room temperature are ideal for efficient separation and reuse. The magnetic properties of the synthesized nanocatalysts were characterized using Vibrating Sample Magnetometry (VSM). As illustrated in Figure 3, the Fe-TiO_2@Fe_3O_4 nanocatalysts demonstrated a maximum saturation magnetization of around 20.5 emu/g. These results confirm that all samples possess superparamagnetic characteristics, facilitating their practical recovery and reuse in catalytic applications.

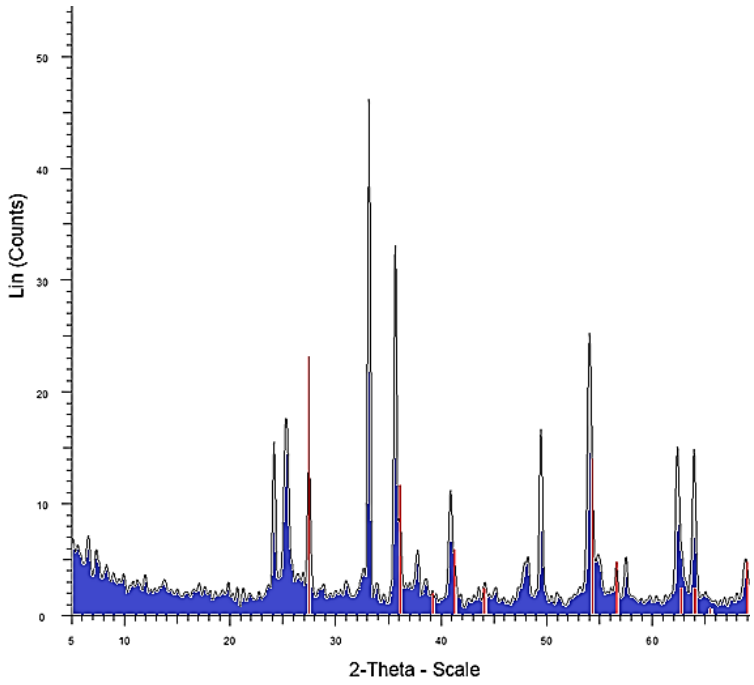

Figure2. The X-ray diffraction spectrum of Fe-doped TiO_2@Fe_3O_4nanocatalysts

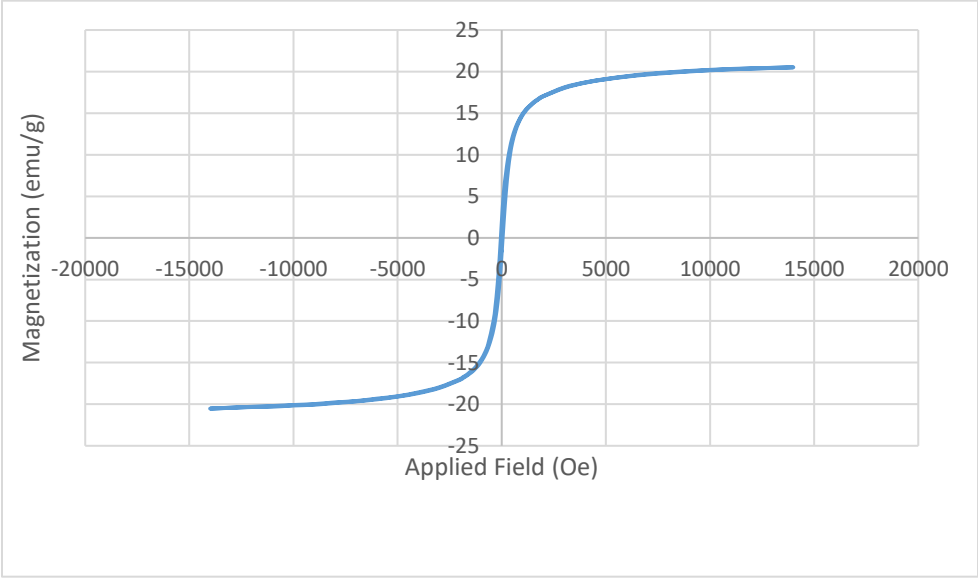

Figure 3. Magnetic properties of the synthesized nanocatalyst sample Fe-doped TiO_2 @ Fe_3O_4

FTIR

Fourier-transform infrared (FTIR) spectroscopy provides a spectrum of the infrared radiation absorbed by a sample, allowing identification of materials based on absorption frequencies and intensities. Figure 4 highlights the characteristic peaks corresponding to functional groups in the Fe-TiO_2@Fe_3O_4 nanocatalysts. The Ti–O–Ti vibrational modes and the bending vibrations of C–H bonds in pure TiO_2 appeared in the ranges of 478.76–685.87

cm^{-1} and 1395.74 cm^{-1}, respectively. Weak absorption bands observed at approximately 2354.55 and 2309.60 cm^{-1} are attributed to the Fe-doped TiO_2 spectrum. A peak at 2926.96 cm^{-1} corresponds to the CH_2 groups from the precursor titanium (IV) isopropoxide. Additionally, absorbance bands at 3429.45 and 1614.65 cm^{-1} are associated with the O–H stretching vibrations and bending vibrations of adsorbed water molecules, respectively (28).

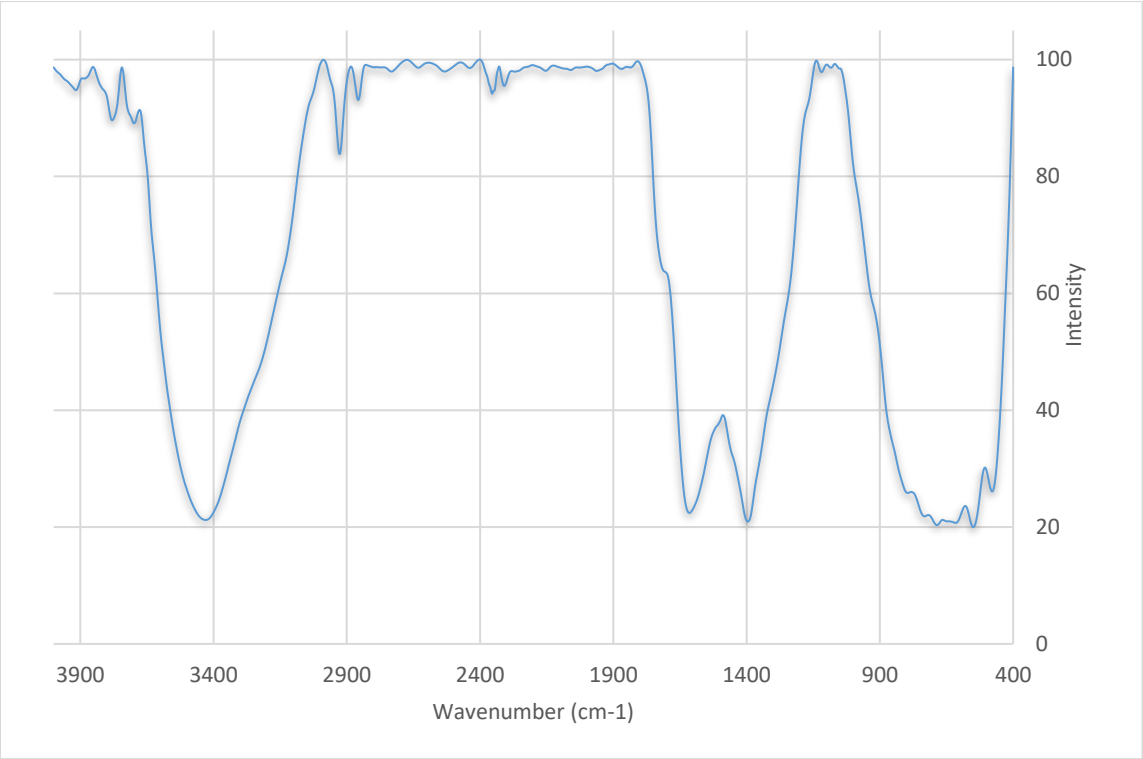

Figure 4. FTIR of Fe-TiO2@Fe3O4 nanocatalysts

Effect of pH

Figure 5 shows the effect of pH on the Azithromycin antibiotic decomposition under acidic, neutral, and basic conditions. The removal efficiency is highly dependent on pH, with acidic conditions favoring higher degradation rates. According to the data, efficiency is 86% at pH 3, 80% at pH 5, 68% at pH 7, 50% at pH 9, and 40% at pH 11 (with 68% efficiency observed at pH 7). In acidic environments, the catalyst surface is positively charged, enhancing electrostatic attraction to Azithromycin molecules and promoting hydroxyl radical generation while minimizing electron-hole recombination. As pH increases to neutral or alkaline levels, the surface becomes negatively charged, leading to repulsion, reduced adsorption, and lower radical production. For maximum removal, pH 3 is optimal, as it maximizes favorable interactions and reactive species formation in the system (29).

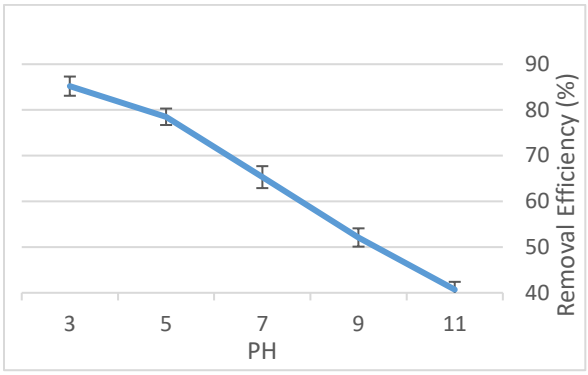

Figure 5. Effect of pH on AZM Removal Efficiency Using Fe-doped $TiO_2@Fe_3O_4$ Nanocatalysts

Effect of Initial Azithromycin Concentration

After determining the optimum pH, the effect of different Azithromycin concentrations was investigated on the removal efficiency. The photocatalytic removal efficiency of Azithromycin using Fe-$TiO_2@Fe_3O_4$ nanocatalysts under UV light decreases as the initial concentration increases (Figure 6). Based on the provided data, at 50 mg/L, the removal efficiency reaches 100%, dropping to 80% at 100 mg/L and further to 60% at 150 mg/L. This trend occurs because higher concentrations lead to saturation of the catalyst's active sites, increased competition among Azithromycin molecules for reactive oxygen species like hydroxyl radicals, and the accumulation of degradation intermediates that can inhibit further reactions. Lower concentrations allow for more effective adsorption and degradation, as there are sufficient active sites and radicals available (5)(30). To maximize removal, the optimal concentration is 50 mg/L, ensuring the highest efficiency without overwhelming the photocatalytic system.

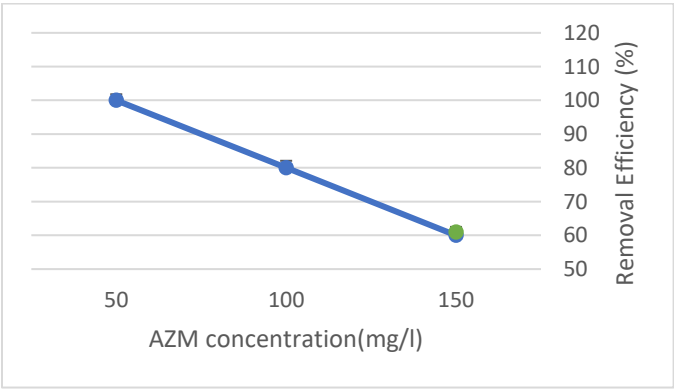

Figure 6. Effect of Initial AZM Concentration on Its Removal Efficiency Using Fe-doped $TiO_2@Fe_3O_4$ Nanocatalysts

Effect of Fe-doped $TiO_2@Fe_3O_4$ dosage

Increasing the catalyst dose initially improves removal efficiency but can lead to a plateau or slight decline beyond an optimal point. The data shows 50% efficiency at 500 mg/L, peaking at 90% at 1000 mg/L, and then decreasing slightly to 85% at 1500 mg/L (Figure 7). At lower doses, there are insufficient active sites for radical generation and pollutant adsorption. Higher doses provide more surface area and reactive sites, but

excessive amounts cause nanoparticle aggregation, increased solution turbidity, and reduced UV light penetration due to scattering (31). The optimal dose for maximization is 1000 mg/L, balancing sufficient catalytic activity with minimal interference to light absorption and overall process efficiency.

Effect of Contact Time

Removal efficiency increases with longer contact time, allowing more opportunities for interactions between Azithromycin and reactive species. From the data, efficiency is 70% at 30 minutes, 90% at 60 minutes, and 95% at 90 minutes (Figure 8). Initially, degradation is rapid due to abundant pollutant availability, but it slows as concentrations decrease and intermediates form. Extended time ensures near-complete degradation without significant catalyst deactivation in this timeframe. The optimal contact time for maximizing removal is 90 minutes, as it provides sufficient duration for the reaction to approach completion, yielding the highest efficiency observed.

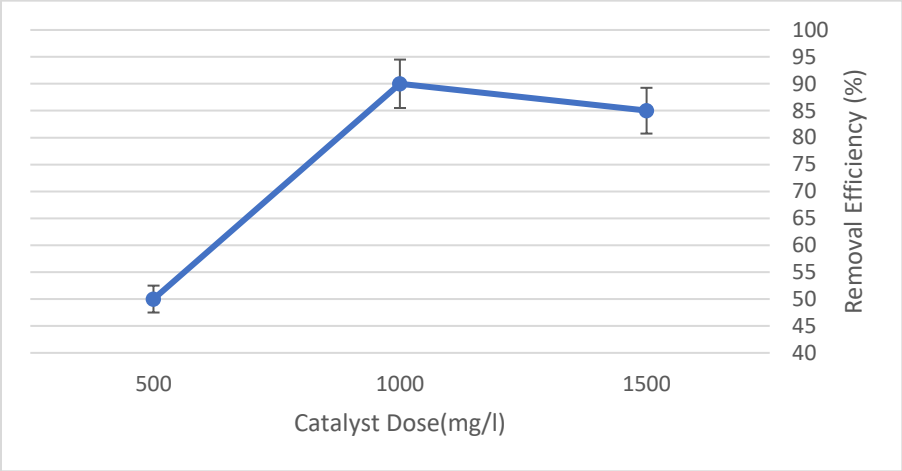

Figure 7. Effect of Fe-doped TiO_2@Fe_3O_4 concentration on photocatalytic degradation efficiency of AZM

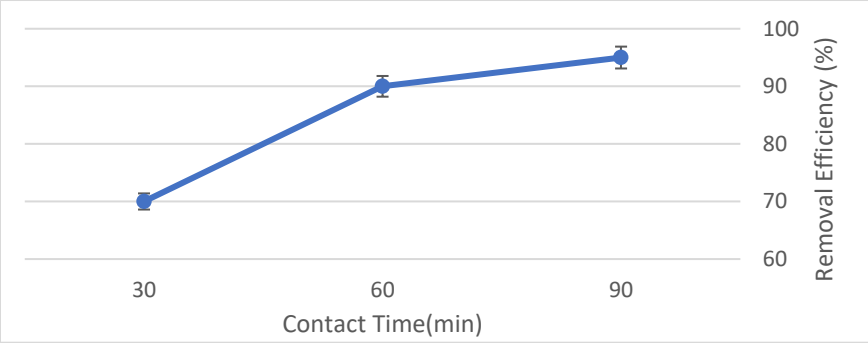

Figure 8. Effect of contact time on the photocatalytic degradation efficiency of AZM Using Fe-doped TiO_2@Fe_3O_4 Nanocatalysts

Conclusion

This study evaluated the efficiency of Azithromycin photocatalytic oxidation from aqueous solutions using synthesized Fe-doped TiO_2@Fe_3O_4 nanocatalysts. The nanocatalysts were prepared via a simple sol-gel method, with characterization confirming the successful incorporation of Fe ions into the TiO_2 nanocomposite structure. The maximum removal efficiency of Azithromycin was achieved using a 30-W UVC lamp, two 15-W lamps with an irradiance of approximately 15mW/cm² under optimal conditions: pH 3, initial Azithromycin concentration of 50 mg/L, catalyst dosage of 1000 mg/L, and a reaction time of 90 minutes. These conditions yielded a removal efficiency of up to 95%, as determined by experimental data. Given the high efficiency of this photocatalytic process, its application is recommended for Azithromycin removal in water purification processes.

Author Contributions: F.H.: methodology, writing—original draft, supervision, investigation, validation.

K: writing—review and editing, supervision, project administration. All authors have read and agreed to the published version of the manuscript.

Funding: This work was supported by the Research Grant of Zahedan University of Medical Sciences, Iran (Grant No: 9797).

Institutional Review Board Statement: Not applicable.

Informed Consent Statement: Not applicable.

Data Availability Statement: The data presented in this research are available on request from the corresponding author.

Conflicts of Interest: The authors declare no conflict of interest

References

1. Kraemer SA, Ramachandran A, Perron GG. Antibiotic pollution in the environment: From microbial ecology to public policy. Microorganisms [Internet]. 2019 Jun 1 [cited 2025 Sep 12];7(6):180. Available from: https://pmc.ncbi.nlm.nih.gov/articles/PMC6616856/

2. Sandman Z, [Internet] OIS, 2024 undefined. Azithromycin. ncbi.nlm.nih.gov [Internet]. [cited 2025 Sep 12]; Available from: https://www.ncbi.nlm.nih.gov/sites/books/NBK557766/

3. Kryazhev A, Maletin D. Therapeutic efficacy of an azithromycin-based drug in calf cryptosporidiosis. BIO Web Conf [Internet]. 2024 Nov 28 [cited 2025 Sep 12];149:01014. Available from: https://www.bio-conferences.org/articles/bioconf/abs/2024/68/bioconf_geneticresources2024_01014/bioconf_geneticresources2024_01014.html

4. Martínez-Polanco MP, Valderrama-Rincón JA, Martínez-Rojas AJ, Luna-Wandurraga HJ, Díaz-Báez MC, Bustos-López MC, et al. Degradation of high concentrations of azithromycin when present in a high organic content wastewater by using a continuously fed laboratory-scale UASB bioreactor. Chemosphere. 2022 Jan 1;287:132191.

5. Hosseinabadi P, Rezaei MR, Sayadi MH, Barani H. Synthesis and photocatalytic degradation of azithromycin by iron/zinc oxide nanoparticle-reinforced carbon nanofibers. Sci Rep [Internet]. 2025 Aug 25 [cited 2025 Sep 12];15(1):1–16. Available from: https://www.nature.com/articles/s41598-025-16849-x

6. Amacher DE, Ellis JH, Joyce AJ, Muehlbauer PA, Turner GN, Wahrenburg MG, et al. Preclinical toxicology studies with azithromycin: genetic toxicology evaluation. Mutat Res Toxicol. 1993 Jul 1;300(2):79–90.

7. Milaković M, Vestergaard G, González-Plaza JJ, Petrić I, Šimatović A, Senta I, et al. Pollution from azithromycin-manufacturing promotes macrolide-resistance gene propagation and induces spatial and seasonal bacterial community shifts in receiving river sediments. Environ Int. 2019 Feb 1;123:501–11.

8. Kalugendo E, Nazir A, Agarwal R. Assessment of azithromycin-induced toxicity in Caenorhabditis elegans: Effects on morphology, behavior, and lipid metabolism. Toxicol Reports [Internet]. 2024 Dec 1 [cited 2025 Sep 12];13:101832. Available from: https://pmc.ncbi.nlm.nih.gov/articles/PMC11664063/

9. Rajak P, Ganguly A, Dey S, Sen K. Antibiotics in wastewater: Exploring the sources, links to antibiotic resistance, and strategies for their removal. Clean Water. 2025 Dec 1;4:100110.

10. Ayach J, El Malti W, Duma L, Lalevée J, Al Ajami M, Hamad H, et al. Comparing Conventional and Advanced Approaches for Heavy Metal Removal in Wastewater Treatment: An In-Depth Review Emphasizing Filter-Based Strategies. Polymers (Basel) [Internet]. 2024 Jul 9 [cited 2025 Sep 12];16(14):1959. Available from: https://www.mdpi.com/2073-4360/16/14/1959/htm

11. Nasir AM, Adam MR, Mohamad Kamal SNEA, Jaafar J, Othman MHD, Ismail AF, et al. A review of the potential of conventional and advanced membrane technology in the removal of pathogens from wastewater. Sep Purif Technol [Internet]. 2022 Apr 1 [cited 2025 Sep 12];286:120454. Available from: https://pmc.ncbi.nlm.nih.gov/articles/PMC8741333/

12. Satyam S, Patra S. Innovations and challenges in adsorption-based wastewater remediation: A comprehensive review. Heliyon [Internet]. 2024 May 15 [cited 2025 Sep 12];10(9):e29573. Available from: https://pmc.ncbi.nlm.nih.gov/articles/PMC11064087/

13. Baskar A V., Bolan N, Hoang SA, Sooriyakumar P, Kumar M, Singh L, et al. Recovery, regeneration and sustainable management of spent adsorbents from wastewater treatment streams: A review. Sci Total Environ. 2022 May 20;822:153555.

14. Kato S, Kansha Y. Comprehensive review of industrial wastewater treatment techniques. Environ Sci Pollut Res 2024 3139 [Internet]. 2024 Aug 7 [cited 2025 Sep 12];31(39):51064–97. Available from: https://link.springer.com/article/10.1007/s11356-024-34584-0

15. Dhamorikar RS, Lade VG, Kewalramani P V., Bindwal AB. Review on integrated advanced oxidation processes for water and wastewater treatment. J Ind Eng Chem. 2024 Oct 25;138:104–22.

16. Mahdi MH, Mohammed TJ, Al-Najar JA. Advanced Oxidation Processes (AOPs) for treatment of antibiotics in wastewater: A review. IOP Conf Ser Earth Environ Sci [Internet]. 2021 [cited 2025 Sep 12];779(1). Available from: https://iopscience.iop.org/article/10.1088/1755-1315/779/1/012109/meta

17. Bhat SA, Sher F, Hameed M, Bashir O, Kumar R, Vo DVN, et al. Sustainable nanotechnology based wastewater treatment strategies: achievements, challenges and future perspectives. Chemosphere. 2022 Feb 1;288:132606.

18. Govan J. Recent advances in magnetic nanoparticles and nanocomposites for the remediation of water resources. Magnetochemistry [Internet]. 2020 Oct 9 [cited 2025 Sep 12];6(4):49. Available from: https://www.mdpi.com/2312-7481/6/4/49/htm

19. Mehmood A, Khan FSA, Mubarak NM, Tan YH, Karri RR, Khalid M, et al. Magnetic nanocomposites for sustainable water purification—a comprehensive review. Environ Sci Pollut Res. 2021 Apr 1;28(16):19563–88.

20. Tripathy J, Mishra A, Pandey M, Thakur RR, Chand S, Rout PR, et al. Advances in Nanoparticles and Nanocomposites for Water and Wastewater Treatment: A Review. Water (Switzerland) [Internet]. 2024 May 23 [cited 2025 Sep 12];16(11):1481. Available from: https://www.mdpi.com/2073-4441/16/11/1481/htm

21. Aragaw TA, Bogale FM, Aragaw BA. Iron-based nanoparticles in wastewater treatment: A review on synthesis methods, applications, and removal mechanisms. J Saudi Chem Soc [Internet]. 2021 [cited 2025 Sep 12];25(8). Available from: https://www.sciencedirect.com/science/article/pii/S1319610321000855

22. Xu W, Yang T, Liu S, Du L, Chen Q, Li X, et al. Insights into the Synthesis, types and application of iron Nanoparticles: The overlooked significance of environmental effects. Environ Int. 2022 Jan 1;158.

23. Ramesh N, Lai CW, Johan MR Bin, Mousavi SM, Badruddin IA, Kumar A, et al. Progress in photocatalytic degradation of industrial organic dye by utilising the silver doped titanium dioxide nanocomposite. Heliyon [Internet]. 2024 Dec 30 [cited 2025 Sep 12];10(24):e40998. Available from: https://pmc.ncbi.nlm.nih.gov/articles/PMC11667620/

24. Anucha CB, Altin I, Bacaksiz E, Stathopoulos VN. Titanium dioxide (TiO_2)-based photocatalyst materials activity enhancement for contaminants of emerging concern (CECs) degradation: In the light of modification strategies. Chem Eng J Adv. 2022 May 15;10:100262.

25. Moein H, Nakhaei S, Norabadi E, Kamani H, Abdipour H. Investigating the photocatalytic removal of amoxicillin from aqueous solutions by Fe-TiO2@Fe3O4 magnetic nanoparticles. Characteristics/effect of parameters/kinetic study. Chem Eng Commun. 2025;212(7):1031–47.

26. Norabadi E, Jahantiq A, Kamani H. Synthesis of Fe-TiO2@Fe3O4 magnetic nanoparticles as a recyclable sonocatalyst for the degradation of 2, 4-dichlorophenol. Environ Sci Pollut Res [Internet]. 2023 Mar 1 [cited 2025 Sep 12];30(11):31446–60. Available from: https://link.springer.com/article/10.1007/s11356-022-24345-2

27. Tan TK, Khiew P, Chiu W, Chia C. Magnetised photocatalyst TiO2/Fe3O4 nanocomposite capable to photodegrade organic dye. IOP Conf Ser Mater Sci Eng [Internet]. 2020 Jan 1 [cited 2025 Sep 12];744(1):012021. Available from:

https://iopscience.iop.org/article/10.1088/1757-899X/744/1/012021

28. Heidarinejad F, Kamani H, Khtibi A. Magnetic Fe-doped TiO2@Fe3O4 for metronidazole degradation in aqueous solutions: Characteristics and efficacy assessment. Heliyon. 2023 Nov 1;9(11):e21414.

29. Mollaie F, Afroomand M, Ahmadi N, Mengelizadeh N, Balarak D. Optimization of photodegradation of acid blue 1 dye on aluminosilicate supported Cu doped TiO2 magnetic nanocatalyst using response surface methodology. Sci Rep [Internet]. 2025 Feb 14 [cited 2025 Sep 12];15(1):1–18. Available from: https://www.nature.com/articles/s41598-025-89968-0

30. Mojahedimotlagh F, Nasab EA, Foroutan R, Ranjbar Vakilabadi D, Dobaradaran S, Azamateslamtalab E, et al. Azithromycin decomposition from simple and complex waters by H2O2 activation over a recyclable catalyst of clay modified with nanofiltration process brine. Environ Technol Innov. 2024 Feb 1;33:103512.

31. Gilbert B, Ono RK, Ching KA, Kim CS. The effects of nanoparticle aggregation processes on aggregate structure and metal uptake. J Colloid Interface Sci. 2009 Nov 15;339(2):285–95.